



NUMERICAL ANALYSIS OF COMPLEX FAILURE MECHANISMS IN COMPOSITE PANELS

Paola Apruzzese*, Brian G Falzon*

*Department of Aeronautics, Imperial College London

Keywords: *Continuum Damage Mechanics, composite structures, implicit FE.*

Abstract

A three-dimensional continuum damage mechanics-based material model has been implemented in an implicit Finite Element code to simulate the progressive degradation of advanced composite materials. The damage model uses seven damage variables assigned to tensile, compressive and non-linear shear damage at a laminae level. The objectivity of the numerical discretization is assured using a smeared formulation.

The material model was benchmarked against experimental uniaxial coupon tests and it is shown to reproduce key aspects observable during failure, such as the inclined fracture plane in matrix compression and the shear band in a $\pm 45^\circ$ tension specimen.

1 Introduction

Strength reduction caused by low velocity impact is one of the principal weaknesses of laminated composite structures. Unlike ductile metals, which can absorb large amounts of energy via plasticity without significant loss of strength, brittle composites absorb energy by elastic deformation and irreversible damage. Impact induced delaminations result in a drastic reduction in strength, stiffness, and stability of the laminate, explaining why impact is of such concern to the designers and users of composite structures. To date, many composite structures are over designed to compensate for their low damage tolerance. The full potential of composite materials has to be yet realised.

Many investigations of impact damage in carbon fibre composites are based on the testing of small laminates rather than structural elements or full-scale structures. These can give comparative data on different fibre/resin systems and different ply lay-ups. However, in addition to the material

properties, other factors can influence the response of a composite structure under impact. These include the geometry of the structure, the local support on substructures and the dynamic response of the structure as a whole.

Validation of structural performance by extensive testing can be prohibitively expensive. Finite element (FE) modelling of impact can replace some of the mechanical testing and thus lead to an improved understanding, and a more efficient design, of components and structures subjected to impact. The present work is intended to develop an in-plane continuum damage model which can be used in combination with interface elements (for the modelling of interlaminar damage) to model the effects of low velocity impacts onto unidirectional (UD) carbon/epoxy and woven/epoxy composite laminates from damage onset to final structural collapse. The final goal being to enable the prediction of impact damage in complex structures, such as composite stiffened panels.

2 Numerical modelling of composite damage

Over the last two decades Continuum Damage Mechanics (CDM) has been employed extensively to describe the progressive degradation experienced by mechanical properties of materials prior to the initiation of macrocracks. The CDM approach, originally developed by Kachanov [1], provides a method which can accurately determine the full range of deterioration in a composite material, from the virgin material, with no damage, to the fully disintegrated material. Material properties over a representative volume are degraded gradually as damage accumulates. Unloading of a damaged structure returns the stress to zero, with a reduced stiffness, while the strain may be fully recovered or reduced to a plastic residual strain [2,3]. For a general and detailed presentation of CDM, the reader is referred to Lemaitre and Chaboche [4].

Recently the basic concepts of CDM have been successfully employed to model the progressive degradation of advanced composite materials. Among others, Iannucci et al. [5] developed and implemented, in the explicit FE code LS-DYNA, a 2D CDM-based model to predict the dynamic response of woven composite laminates under impact loading. Successively, Donadon [6] improved and extended that model to include 3D effects. In contrast, the models, available in the literature, that make use of an implicit solver are either based on the assumption of plane stress or consider a single isotropic damage variable. 3D anisotropic damage models are, to the authors' knowledge, only available for explicit FE code and have been applied to plates or other simple geometries as CPU requirements increase dramatically for complex geometries.

The present model is implemented within an implicit FE code and is not based on the assumption of plane stress; it allows for a full 3D stress analysis to be carried out, which is essential for modelling impact damage. While this difference is not readily appreciable when the fibre fracture in tension is investigated, it becomes noticeable when matrix fracture and fibre fracture in compression (microbuckling and fibre kinking) are considered. Another feature of the present model is that according to experimental evidence, the shear behaviour, in all of the three shear directions is markedly non-linear and irreversible, even before the localization process.

3 Constitutive damage model

This section describes in detail the 3D energy based damage model developed and implemented in the implicit finite element code ABAQUS/Standard [7] by the user subroutine UMAT.

3.1 Effective stress-stain relationship

In CDM models a fictitious effective stress $\tilde{\sigma}$ is introduced. This fictitious stress acts on an effective resisting area (A_{ef}), which represents a reduction of the original area A due to material degradation caused by the presence of microcracks and stress concentration in the vicinity of cracks. In general form, the effective stress $\tilde{\sigma}$ is related to the actual Cauchy stress σ in the undamaged material using the damage effect tensor M , as,

$$\sigma = M \tilde{\sigma}. \quad (1)$$

Different hypotheses based on equivalence of strain or elastic energy have been proposed to evaluate M and hence establish a relation between the damaged and undamaged stiffness. Lemaitre and Chaboche [4] proposed the "principle of strain equivalence" which states:

"any deformation behaviour, whether uniaxial or multiaxial, of a damaged material is represented by the constitutive laws of the virgin material in which the usual stress, σ , is replaced by the effective stress, $\tilde{\sigma}$."

Accordingly, for example the uniaxial linear elastic law of a damaged material is written as,

$$\varepsilon = \frac{\tilde{\sigma}}{E} = \frac{\sigma}{(1-d)E}, \quad (2)$$

where E is the Young's modulus of the virgin material and d is the damage parameter. Based on this principle the compliance relationship for orthotropic elastic material can be expressed in terms of effective stress $\tilde{\sigma}$ as,

$$\tilde{\sigma} = H_0^{-1} \varepsilon, \quad (3)$$

where H_0^{-1} is the inverse of the compliance matrix of the undamaged lamina. Combining Eq. (1) and (3) results in a constitutive equation expressed by,

$$\sigma = M H_0^{-1} \varepsilon. \quad (4)$$

These basic concepts are used to develop a damage model with seven different damage variables (d_i) introduced to take into account typical mechanisms of fracture of composite laminate. These are fibre fracture in tension (d_1^t) and compression (d_1^c), matrix failure in tension (d_2^t) and compression (d_2^c) and three other damage variables to account for non-linear shear behaviour and irreversibility (d_{12} , d_{13} , d_{23}). Each damage variable is a monotonically increasing function such that $0 \leq d_i \leq 1$ (where $d=0$ represents the initial undamaged material and $d=1$ represents a state of complete loss of integrity, in which no stresses can be transferred) and is activated by a specific physically-based failure criterion. Once a failure criterion has been exceeded, the stresses are degraded following a linear softening law.

4 Damage criteria

The determination of the domain of elastic response under a complex stress state is an essential component for an accurate damage model. The failure envelope is determined by four damage

activation functions associated with damage in the longitudinal and transverse directions. These damage activation functions are defined as,

$$F_i^{t,c} = f_i^{t,c} - r_i^{t,c}, \quad (5)$$

where $f_i^{t,c}$ are the failure criteria, which depend on the stress/strain tensors and the material properties, and $r_i^{t,c}$ is the elastic domain threshold.

The elastic domain threshold defines the amount of elastic strain that can be applied to the material before further damage is accumulated. It assumes initially the value 1 for the undamaged material and then increases with the damage.

In the following, the subscript 1 refers to the fibre direction, the subscript 2 refers to the in-plane transverse direction and the subscript 3 refers to the through-thickness direction. The superscript t and c refer to tensile and compressive failure criteria, respectively.

4.1 Fibre tensile failure

Since the stresses in fibre direction are predominantly transmitted through the fibre because of their high stiffness and strength in comparison to the matrix properties, the damage initiation due to tensile loading in longitudinal direction is predicted using a non-interacting strain based failure criterion. The resultant damage activation function is given by,

$$F_{11}^t(\varepsilon_{11}) = \left(\frac{E_1}{X_T} \varepsilon_{11} \right)^2 - r_{11}^t \geq 0, \quad (6)$$

where r_{11}^t is the elastic domain threshold and is given by,

$$r_{11}^t(\tau) = \max_{\tau} \left(1, \left(\frac{E_1}{X_T} \varepsilon_{11} \right)^2 \right), \quad (7)$$

where E_1 is the Young's modulus in the longitudinal direction and X_T is the axial tensile strength. In Eq.(7) τ represents the fictitious time that distinguishes each load increment during the FE analysis.

When this criterion is fulfilled, the material properties are degraded to account for the damage in the structure. The damage variable d^t is defined in this model to linearly degrade the respective Young's modulus E_l and Poisson's ratio ν_{12} . This

damage variable is defined so that it has the value 0 at onset of failure, where $\varepsilon_{11} = \varepsilon_{11}^0$, and the value 1 at final failure ($\varepsilon_{11} = \varepsilon_{11}^f$), Fig.1.

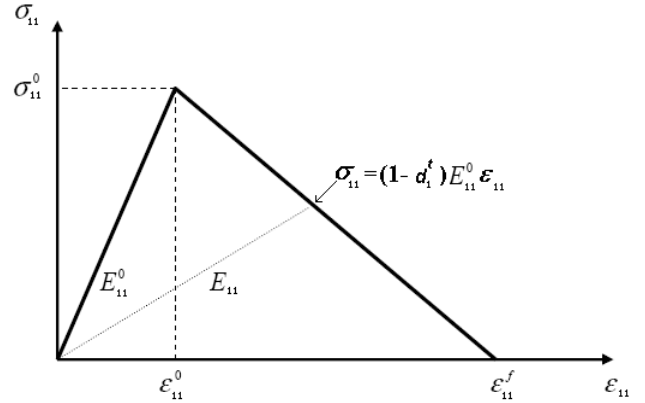


Fig.1. Constitutive law in tension

The bilinear damage evolution law can then be expressed in the following general form,

$$d_1^t = \frac{\varepsilon_{11}^f - \varepsilon_{11}^0}{\varepsilon_{11}^f - \varepsilon_{11}^0} \left(1 - \frac{\varepsilon_{11}^0}{\varepsilon_{11}} \right). \quad (8)$$

4.2 Fibre compressive failure

In the present formulation fibre kinking is formulated in a similar manner to the tensile failure. Once an initiation (failure) strain is reached, damage initiates and stress is gradually reduced to the residual strength value, typically the crushed fibre strength. As an initial estimate, this was taken as the matrix strength. This allows the kink or matrix crush zone to have a residual strength, unlike the tensile failure modes. An extension of this model, suggested by Iannucci et al., in [5], would introduce a further compressive final failure strain to take into account the energy dissipated due to plastic deformation of the crushed zone.

A strain based criterion is assumed as the damage activation function. This is given by,

$$F_{11}^c(\varepsilon_{11}) = \left(\frac{\varepsilon_{11}}{\varepsilon_{11}^0} \right)^2 - r_{11}^c \geq 0, \quad (9)$$

where ε_{11}^0 is the initial failure strain in compression and r_{11}^c is the elastic domain threshold which is given as,

$$r_{11}^c(\tau) = \max \left(1, \left(\frac{\varepsilon_{11}}{\varepsilon_{11}^0} \right)^2 \right). \quad (10)$$

The damage growth law assumes a similar form to that used for predicting failure in tension,

$$d_{11}^c = \frac{\varepsilon_{11}^f}{\varepsilon_{11}^f - \varepsilon_{11}^0} \left(1 - \frac{\varepsilon_{11}^0}{\varepsilon_{11}} \right), \quad (11)$$

where ε_{11}^f is the strain at final failure.

As discussed above, in order to model matrix crushing and fragment interaction effects within the crushing zone of the material, the stress σ_{11} is not completely degraded but is reduced to a minimum residual stress which is assumed comparable to the transverse compressive strength of matrix, σ_{11}^{res} . The resultant stress-strain behaviour in compression is shown in Fig.2.

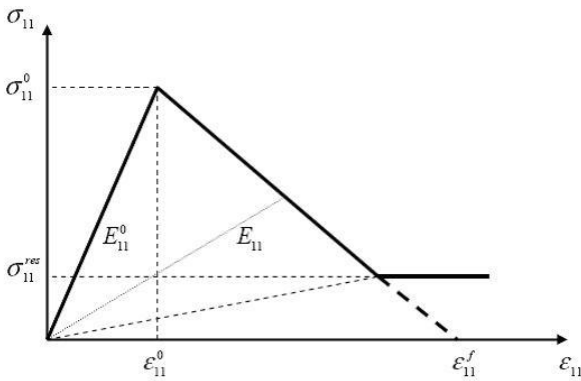


Fig.2. Constitutive law for fibre in compression

4.3 Matrix failure

4.3.1 Failure criteria

Experimental evidence on the fracture surface of specimens failing by matrix compression suggests that unidirectional layers behave in a very brittle manner at failure. Following this observation, Puck and Schneider [8], formulated a failure criterion for matrix failure based on the Mohr-Coulomb criterion. The fundamental hypothesis on which the Puck's criterion is based is that the fracture is exclusively created by the stresses which act on the fracture plane. In the case of inter-fibre fracture on an inclined plane parallel to the fibre these stresses are the normal stress σ_n , and two shear stresses τ_{nl} and τ_{nt} as shown in Fig.3.

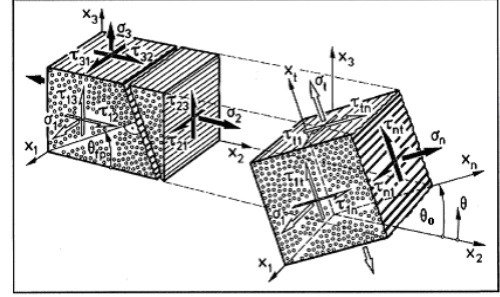


Fig.3. Schematic representation of the fracture plane

The stress σ_n represents the stress perpendicular to the fracture plane (σ_{\perp}), the shear τ_{nl} is the transverse-longitudinal shear stress $\tau_{\perp\parallel}$ and τ_{nt} is the transverse-transverse shear stress $\tau_{\perp\perp}$.

When $\sigma_n \geq 0$ the fracture criterion can be easily stated as,

$$\left(\frac{\sigma_n}{R_{\perp}} \right)^2 + \left(\frac{\tau_{nt}}{R_{\perp\perp}} \right)^2 + \left(\frac{\tau_{nl}}{R_{\perp\parallel}} \right)^2 \geq 1, \quad (12)$$

where R_{\perp} , $R_{\perp\perp}$, and $R_{\perp\parallel}$ are the strengths related to the fracture plane. In particular for $\sigma_n \geq 0$ the fracture angle (θ) reduces to 0° degrees and therefore R_{\perp} , $R_{\perp\perp}$, and $R_{\perp\parallel}$ reduce to Y_T , S_L and S_T , which are transverse tensile strength, in-plane shear strength and out-of plane shear strength, respectively.

Applying this criterion to predict transverse tensile matrix fracture results in a damage activation function that read as,

$$F_{22}^t = \left(\frac{\tilde{\sigma}_2}{Y_T} \right)^2 + \left(\frac{\tilde{\tau}_{12}}{S_L} \right)^2 + \left(\frac{\tilde{\tau}_{23}}{S_T} \right)^2 - r_{22}^t \geq 0. \quad (13)$$

While for $\sigma_n > 0$ the angle of the fracture plane is always assumed equal to 0° , the same cannot be asserted when $\sigma_n < 0$ and consequently the strengths related to the fracture plane are hardly available. Based on the experimental evidence that a tensile stress $\sigma_n > 0$ promotes fracture, whereas a compressive stress $\sigma_n < 0$ impedes shear fractures, Puck concluded that for $\sigma_n < 0$ the shear stresses τ_{nt} and τ_{nl} have to cause fracture against an additional resistance, which increases with increasing $|\sigma_n|$ like an "internal friction". This idea has been developed further by Davila and al. in the LaRC04 failure criteria [9-10]. The proposed fracture criterion for matrix in compression is given by,

$$\left(\frac{\tilde{\tau}_{nt}}{S_T - \mu_T \tilde{\sigma}_n}\right)^2 + \left(\frac{\tilde{\tau}_{nl}}{S_L - \mu_L \tilde{\sigma}_n}\right)^2 \geq 1 \quad \text{for } \sigma_n < 0, \quad (14)$$

where $\mu_T = \frac{1}{\tan(2\theta_0)}$ and $\mu_L = S_L \frac{\mu_T}{S_T}$ are

referred to as ‘‘friction coefficients’’, and θ_0 is the angle of the fracture plane for pure compression in the direction perpendicular to the fibre that usually assumes a value $\approx 53^\circ$. These ‘‘friction coefficients’’ have been used by previous authors [8] even though there is no real friction, at least, not until the fracture surfaces are created.

For a general loading situation, the angle of the fracture plane with the through-the-thickness direction might assume a different value than the one for pure compression ($\approx 53^\circ$). However, in the present model we assume that the fracture angle can only take two discrete values: 0° (for $\sigma_n > 0$) or 53° ($\sigma_n < 0$). Applying this fracture criterion to predict transverse compressive matrix fracture results in a damage activation function that reads as,

$$F_{22}^c = \left(\frac{\tilde{\tau}_{nt}}{S_T - \mu_T \tilde{\sigma}_n}\right)^2 + \left(\frac{\tilde{\tau}_{nl}}{S_L - \mu_L \tilde{\sigma}_n}\right)^2 - r_{22}^c \geq 0. \quad (15)$$

4.3.2 Damage evolution

Due to the fundamental hypothesis that the fracture is exclusively created by the stresses acting on the fracture plane (*Int*), see Fig.4, the transverse compression fracture criterion requires that the ‘‘effective stress tensor’’, $\tilde{\sigma}$ (namely the stress tensor acting on the cross-sectional area effectively resisting the loading ($A - A_{\text{damaged}}$)) has to be rotated into the fracture coordinate system, using the standard tensor transformation rules.

If the rotated stress components satisfy one of the damage activation functions Eq.13 or Eq.15, depending on the sign $\tilde{\sigma}_n$, the stress components of the effective stress tensor ($\tilde{\sigma}_{Int}$) acting on the fracture plane have to be degraded as,

$$\sigma_n = (1 - d_2^{t,c}) \frac{\langle \tilde{\sigma}_n \rangle}{\tilde{\sigma}_n} \tilde{\sigma}_n, \quad (16a)$$

$$\tau_{nl} = (1 - d_2^{t,c}) \tilde{\tau}_{nl}, \quad (16b)$$

$$\tau_{nt} = (1 - d_2^{t,c}) \tilde{\tau}_{nt}, \quad (16c)$$

where $d_2^{t,c}$ is the damage variable, which evolves following the evolution law,

$$d_2^{t,c} = \frac{\varepsilon_{MAT}^f}{\varepsilon_{MAT}^f - \varepsilon_{MAT}^0} \left(1 - \frac{\varepsilon_{MAT}^0}{\varepsilon_{MAT}}\right), \quad (17)$$

where $\varepsilon_{MAT} = \sqrt{\langle \varepsilon_n \rangle^2 + \gamma_{nt}^2 + \gamma_{nl}^2}$ represents the total shear component acting on the fracture plane, ε_{MAT}^0 and ε_{MAT}^f are the shear strains at the onset of damage and at failure ($d_2 = 1$), respectively, as shown in Fig.7.

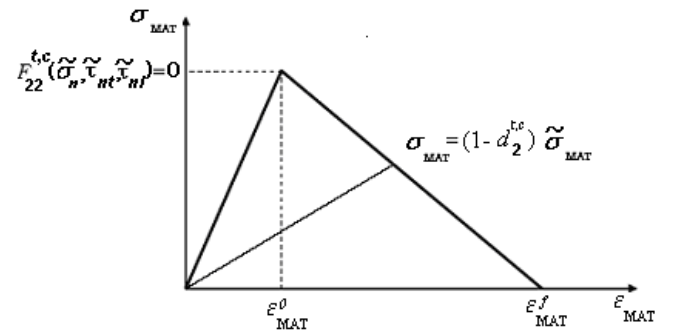


Fig.4. Local model behaviour for transverse failure

In the above figure (Fig.4)

$\sigma_{MAT} = \sqrt{\langle \sigma_n \rangle^2 + \tau_{nt}^2 + \tau_{nl}^2}$ represents the driving stress acting on the fracture plane and it corresponds to the total strain components which actually ‘drives’ the damage evolution. In a more general form the true Cauchy stress tensor (σ_{Int}), acting on the whole area (A), can be expressed as,

$$\sigma_{Int} = M_{Int} (d_2^{t,c}) \tilde{\sigma}_{Int}, \quad (18)$$

where M_{Int} is the damage tensor.

In the fracture coordinate system (*Int*) the damage tensor is a diagonal tensor but, in general, this condition no longer holds once this tensor is rotated back into the lamina coordinate system.

5 Non linear shear-stress behaviour

According to experimental evidence, the shear behaviour of composite materials, in each of the three shear directions, is markedly non-linear and irreversible. In general the non-linear material behaviour of composites is ascribed to two distinct mechanical processes: plasticity and loss of stiffness due to progressive damage. A number of different

approaches to the modelling of the shear behaviour can be found in the literature. Degradation phenomena have been described, in the literature, by either continuum theories of plasticity [11], continuum damage mechanics [4] or combining both theories [12].

In the present formulation we adopt the shear model proposed by Donadon [6]. A polynomial cubic stress-strain relationship is used to represent the non-linear behaviour in shear which is given by,

$$\tau_{ij}(\gamma_{ij}) = c_1 \gamma_{ij}^3 - c_2 \cdot \text{sign}(\gamma_{ij}) \cdot \gamma_{ij}^2 + c_3 \gamma_{ij}, \quad (19)$$

where c_1 , c_2 and c_3 are coefficients determined by fitting the polynomial expression to experimentally obtained stress-strain curves.

Two state variables are introduced: the shear damage d_{ij} and the permanent inelastic strain γ_{ij}^{in} . A strain based criterion is assumed for the damage activation function that read as,

$$F_{ij}^{Shear}(\gamma_{ij}) = \left(\frac{\gamma_{ij}}{\gamma_{ij}^0} \right)^2 - r_{ij}^n \geq 0, \quad (20)$$

where γ_{ij}^0 is the maximum allowable elastic strain and r_{ij}^n is the elastic domain threshold which is given by,

$$r_{ij}^n(\tau) = \max_{\tau} \left\{ 1, \left(\frac{\gamma_{ij}}{\gamma_{ij}^0} \right)^2 \right\}. \quad (21)$$

After detecting shear damage initiation, the damage evolution is defined by a bi-phase law (strain based). The first damage phase, curve OA in Fig.5, is associated with the gradual stiffness reduction due to matrix microcracking while the second phase, curve AB in Fig.5, represents the loss of load carrying capability in shear as the fracture energy in shear is dissipated.

The damage evolution law is given by,

$$d_{ij} = \lambda_1(\gamma_{ij}) + \lambda_2(\gamma_{ij}) - \lambda_1(\gamma_{ij}) \lambda_2(\gamma_{ij}), \quad (22)$$

where the functions $\lambda_1(\gamma_{ij})$ and $\lambda_2(\gamma_{ij})$ are defined as follows,

$$\text{for } \gamma_{ij}^0 \leq \gamma_{ij} \leq \gamma_{ij}^{\max} \implies \lambda_1 = a \gamma_{ij} \text{ and } \lambda_2 = 0$$

$$\text{while for } \gamma_{ij}^{\max} \leq \gamma_{ij} \leq \gamma_{ij}^f \implies$$

$$\lambda_1 = a \gamma_{ij}^{\max} \text{ and } \lambda_2 = \frac{\gamma_{ij}^f}{\gamma_{ij}^f - \gamma_{ij}^{\max}} \left(1 - \frac{\gamma_{ij}^{\max}}{\gamma_{ij}} \right),$$

where γ_{ij}^f and γ_{ij}^{\max} are the failure strain and the

maximum strain, respectively. $a = \left| \frac{\Delta(G_{ij} \setminus G_{ij0})}{\Delta \gamma_{ij}} \right|$ is

a material constant which expresses the gradual shear stiffness (G_{ij}) reduction obtained in cyclic loading-unloading shear testing using $(+45/-45)_n$ specimens.

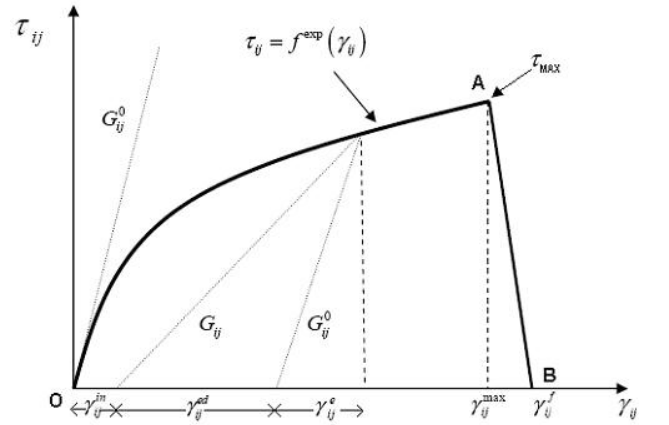


Fig.5. Constitutive model in shear

Assuming small strain hypothesis, the total strain can be additively decomposed into elastic γ_{ij}^e and damage γ_{ij}^d parts,

$$\gamma_{ij} = \gamma_{ij}^e + \gamma_{ij}^d.$$

Although the damage process is irreversible thermodynamically, the deformation due to damage itself can be partially or completely recovered upon unloading. Thus, the damage strain component can also be decomposed into elastic (reversible), γ_{ij}^{ed} , and inelastic (irreversible), γ_{ij}^{in} , parts,

$$\gamma_{ij}^d = \gamma_{ij}^{ed} + \gamma_{ij}^{in}. \quad (23)$$

During the unloading process only the elastic strain γ_{ij}^e and the elastic-damage strain γ_{ij}^{ed} are totally recovered. The shear stress during unloading can be defined as,

$$\text{for } |\bar{\gamma}_{\max}| > |\gamma_{ij}| > |\gamma_{ij}^{in}|,$$

$$\tau_{ij} = \frac{\gamma_{ij}}{|\gamma_{ij}|} G_{ij}^0 (1 - d_{ij}) \left(|\gamma_{ij}| - |\gamma_{ij}^{in}| \right), \quad (24a)$$

where $\bar{\gamma}_{\max} = \max_i |\gamma_{ij}|$ and for $|\gamma_{ij}| < |\gamma_{ij}^{in}|$,

$$\tau_{ij} = 0. \quad (24b)$$

The accumulation of the permanent shear strain, γ_{ij}^{in} , is assumed to depend on the total shear strain and the damage variable as follows,

$$\gamma_{ij}^{in} = \gamma_{ij} - (\gamma_{ij}^e + \gamma_{ij}^{ed}) = \gamma_{ij} - \left(\frac{\tau_{ij}}{G_{ij}^0} + \frac{\tau_{ij} \cdot d_{ij}}{G_{ij}^0 \cdot (1 - d_{ij})} \right). \quad (25)$$

6 Smearred formulation

Strain localization is a major problem in the FE model of softening material behaviour, such as that induced by the damage. As damage grows in a finite element, the material stiffness degrades to zero and the deformation tends to infinity. The energy dissipation is consequently dependent on the discretization size. The simplest, but crudest, way to obtain objectivity is modifying the constitutive law and making it depend on the mesh size by introducing a parameter called ‘‘crack band width’’ [13] or ‘‘characteristic length’’. For the sake of simplicity, in the present model the objectivity of the solution is obtained using the ‘‘crack band model’’ [13] that assume that the fracture energy of the material, g_f , is distributed (smeared) over the full volume of the element. A length characteristic of the finite element is then introduced to correlate fracture toughness, G_M , and energy dissipated per unit volume,

$$g_M = \frac{G_M}{l^*}. \quad (26)$$

Accordingly, the area under the uniaxial stress-strain curve is adjusted by expressing the maximum allowable strain ε_f as a function of the fracture energy per unit of cracked area, G_f , material strength, σ^0 , and the characteristic element length, l^* ,

$$\varepsilon_f = \frac{2G_f}{\sigma^0 l^*}, \quad (27)$$

when ε_f is defined by Eq.27 the energy absorbed per unit of cracked area is independent of the mesh refinement.

6.1 Critical element size

From Eq.27 one can deduce that when for a very coarse mesh ($l^* \rightarrow \infty$), ε_f tends to zero. This is inadmissible behaviour, as it would mean that the element absorbs more elastic energy at failure onset (from zero strain to ε_0) than the energy absorbed for the fracture process (from ε_0 to ε_f). Therefore in order to prevent this inconsistency a maximum characteristic element length has been defined,

$$l^* \leq \frac{\sigma_0 \varepsilon^0}{2G_f}. \quad (28)$$

7 Computational algorithm material model

The material behaviour outlined in the previous section is implemented using the commercial FE code ABAQUS by means of the user defined material subroutine UMAT. This subroutine is called at all material calculation points of elements for which the material definition includes a user defined material behaviour.

The iteration for global equilibrium of a system is performed using the Newton–Raphson method. The applied scheme is iteration independent, which means that all variables are only updated at the end of an increment step after convergence is achieved. The task to be performed by the user-supplied routine is to integrate physical relations at a point level (Gauss point of an element) when starting from a known equilibrium state and for a total strain increment given in each iteration. The output information is stress and all other state variables are updated (integrated) by the end of the iteration increment. At each load increment, a nonlinear system of equations must be solved; to do so with the Newton-Raphson method and achieve quadratic convergence, the consistent tangent matrix must be used.

The tangent stiffness matrix can be expressed as,

$$C_T = \frac{\partial \Delta \sigma}{\partial \Delta \varepsilon}, \quad (29)$$

where $\Delta \sigma$ are the stress increments and $\Delta \varepsilon$ are the strain increments.

In particular, $C_T(i, j)$ represents the change in the i -th stress component at the end of the time increment caused by an infinitesimal perturbation of the j -th component of the strain increment array. The constitutive equation defined in Eq.4 can be written as,

$$\sigma = M_{tot} \tilde{\sigma} = M_{tot} C \varepsilon, \quad (4bis)$$

where C is the stiffness matrix of the undamaged material, and M_{tot} can be expressed as,

$$M_{tot} = RM_{LNT}(d_2^c) M_{123}(d_1^{tc}, d_2^t, d_{12}, d_{13}, d_{23}), \quad (30)$$

where RM_{LNT} is the damage tensor accounting for matrix fracture in compression, rotated in the principal coordinate system and M_{123} is the damage tensor accounting for the other forms of damage. In general form the tangent stiffness matrix to compute at the end of each step increment is given by,

$$C_T = \frac{\partial \Delta \sigma}{\partial \Delta \varepsilon} = M_{tot} C + \frac{\partial M_{tot}}{\partial d_i} \frac{\partial d_i}{\partial \varepsilon} C \varepsilon. \quad (31)$$

The resultant tangent stiffness matrix is not symmetric. However, in order to improve the computational efficiency without affecting the accuracy of the solution a symmetric matrix storage scheme was used.

7.1 Convergence of the Newton-Raphson method

In the literature, several authors use explicit dynamic FE codes to deal with strain softening behaviour [5,6,14]. Using explicit methods a solution is easily achieved, provided that sufficient small increment sizes are used. Moreover, for explicit FE codes, the failure location is defined by both rounding errors in terms of strength within the elements and wave reflection effects within the FE mesh. These two effects acting simultaneously define a band of failed elements which mimic the fracture of the real structural component [6].

In contrast, using an implicit solution algorithm the localization has to be introduced artificially. There is no wave reflection effect within the FE mesh, hence when uniform displacement is applied at the ends of a plate with no cuts or holes, a constant stress field is generated. The constant stress field implies a uniform strain field which does not produce localization. A general practice to trigger fracture localization is to introduce an imperfection in the numerical model. In all the example that follow, an element with slightly lower strength

(typically 10%) was used to trigger the failure location.

Strain-softening constitutive models may cause convergence difficulties when using global solution methods. When strong instabilities prevent the convergence of the Newton-Raphson method the introduction of a small damping force facilitates a rapid convergence to a consistent solution. These damping forces can be easily introduced in ABAQUS\Standard using the ‘Stabilize method’ [7].

8 Applications

This section presents some applications of the damage model implemented. Each failure model has been tested on simple one element test cases to assess the correctness of the numerical implementation, for brevity, the results are omitted.

8.1 Mesh sensitivity

In order to assess the mesh sensitivity of the damage model implemented, a simple tensile test has been carried on a cube of volume 1mm^3 made of carbon-epoxy T300/913. The specimen was subjected to uniform displacement along the fibre direction. The material properties are reported in Table1. The mesh densities tested were 1mm, 0.5 mm, 0.25 mm and 0.125mm.

E_1 (GPa)	$E_2=E_3$ (GPa)	$G_{12}=G_{31}$ (GPa)	ν_{23}	$\nu_{12}=\nu_{13}$	G_f (N/mm)	X_t (MPa)
132	8.8	4.6	0.4	0.315	91.7	2005

Table 1. Material properties T300\913 [14]

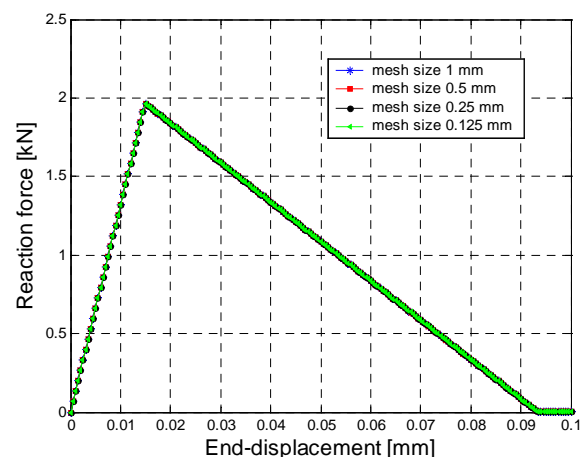


Fig.6. Mesh sensitivity

The load-displacement responses for all meshes are plotted in a single graph, Fig.6. The structural responses obtained using different meshes

are almost identical which ensures the control of energy dissipation regardless of mesh refinement. From Fig.6 it is straightforward evaluating the energy dissipated during fracture which is defined by the area underneath the force-displacement curve.

8.2 In-plane coupon tests simulation

The material model was benchmarked against experimental uniaxial coupon tests taken from [6]. For brevity, only the results of two of the most significant tests are reported herein. The tests were carried out on woven CFRP specimens. The material properties used in FE analyses are reported in Table 2. Each simulation was carried out using 8 node reduced integration solid elements (C3D8R) with enhanced hourglass stiffness.

E_1 (GPa)	$E_{2,3}$ (GPa)	$G_{12,23,31}$ (GPa)	ν_{12}	X_T (MPa)	Y_T (MPa)	Y_C (MPa)	S_{12} (MPa)
100.	8.11	3.88	0.33	2000	74.1	160.	61

C_1 (Eq.19)	C_2 (Eq.19)	C_3 (Eq.19)	G_{f11}^I (N/mm)	G_{f22}^I (N/mm)	G_{f12} (N/mm)
2.0E6	164.6E3	5.06E3	160.	2.25	2.25

Table 2. Material properties and fracture toughness

8.2.1 Modelling matrix compressive failure

The FE model for uniaxial transverse compression had the dimension of 10x10x2.25 mm (LxWxT) and $[90^\circ]_5$ layup. Each ply, with a nominal thickness of 0.45mm, was modelled using 3 solid elements per layer. The fracture angle measured in the pure transverse compression test was 45° , consequently this value was used in the FE simulation. The angle of the band of failed element, which can be observed in Fig.7 is also $\approx 45^\circ$. The results obtained, agree well with the experiments as shown in Fig.8

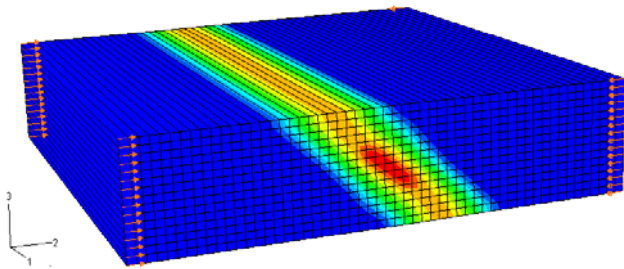


Fig.7. Band of failed elements

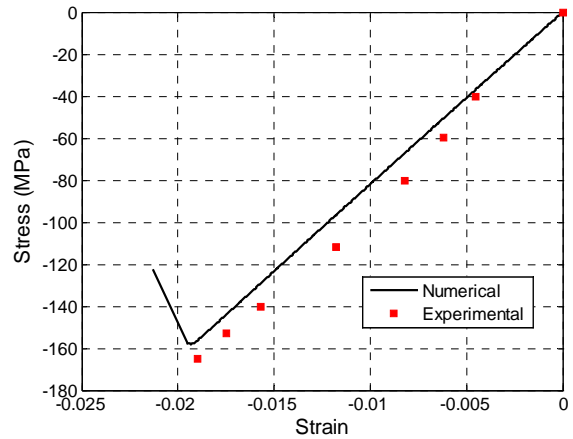


Fig.8. Transverse stress –strain response in compression

8.2.2 Modelling shear failure

The virtual coupon test for in-plane shear testing has dimensions 100x20x2.7mm (LxWxT) and $(+45^\circ/-45^\circ)_3$ layup. The model had 6 solid elements across the thickness to simulate each layer individually. Fig.9 shows the formation of the shear band pairs that initiate at two location.

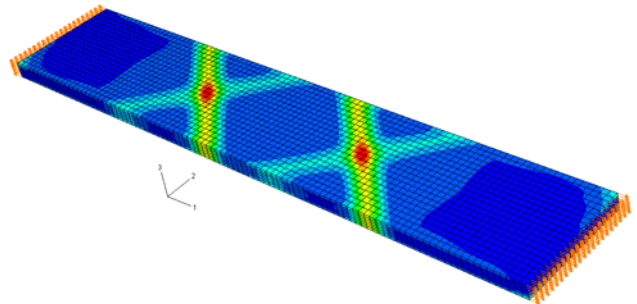


Fig.9. Shear band at damage initiation

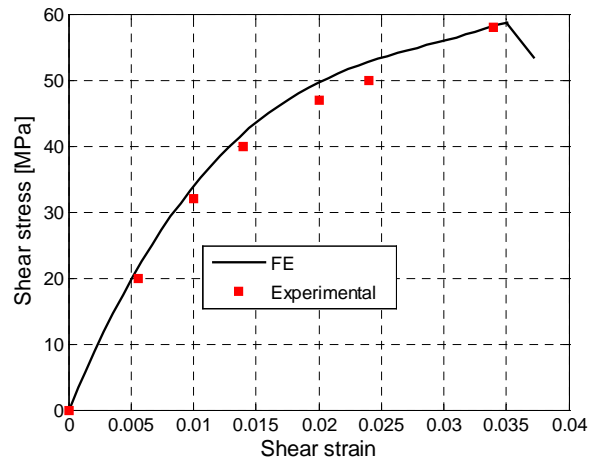


Fig.10. Experimental and numerical shear stress-strain curve

The numerical shear stress vs. shear strain curve is compared to the experiment in Fig.10.

9 Conclusions

A 3D constitutive material model for the prediction of damage onset, growth and ultimate failure was developed and implemented in the non-linear FE code ABAQUS. The full non-linear stress-strain relation for a lamina in shear is considered.

The model was validated against experimental data for in-plane coupon tests and it is shown to reproduce key aspects observable during failure, such as the inclined fracture plane in matrix compression and the shear band in $\pm 45^\circ$ tension specimen.

The success of the present methodology is promising and points the way for extending its application to more complex structural configurations.

Acknowledgements

The authors would like to acknowledge the financial support of QinetiQ through contract No. CU004-27274.

References

- [1] Kachanov, L.M. “*Introduction to Continuum Damage Mechanics*”. M. Nijhoff, Boston, Dordrecht, 1987
- [2] Edlund U, Klarbring A. “A coupled elastic–plastic damage model for rubber-modified epoxy adhesives”. *Int J Solid Struct.*, Vol. 30, No. 19, pp 2693–708, 1993.
- [3] Siron O, Pailhes J, Lamon J. “Modelling of the stress/strain behaviour of a carbon/carbon composite with a 2.5 dimensional fibre architecture under tensile and shear loads at room temperature”. *Compos Sci Technol*, Vol.59,No.1,pp 1–12, 1999.
- [4] Lemaitre, J., Chaboche, J.L. “*Mechanics of Solids*”. Cambridge University Press, 1990.
- [5] L.Iannucci, J. Ankersen. “An energy based damage model for thin laminated composites”. *Composite Science and Tech.*, Vol. 66, pp 934-951, 2006.
- [6] M.V. Donadon. “*The structural behaviour of composite laminates manufactured using resin infusion under flexible tooling*”. PhD Thesis, Department of Aeronautics, Imperial College London, 2005.
- [7] ABAQUS finite element system V6.5-1, Hibbit, Karlsson and Sorensen Inc, 2004.
- [8] Puck A, Schurmann H. “Failure analysis of FRP laminates by means of physically based phenomenological models”. *Comp Sci Technol*, Vol.58, pp 1045–67, 1998.
- [9] Dávila C. G., Camanho P. P., Rose C. A. “Failure criteria for FRP laminates” *Journal of Composite Materials*, Vol. 39 pp 323-345, 2005.
- [10] Pinho S. T., Dávila C. G. Camanho P. P., Iannucci L., Robinson P. “Failure models and criteria for FRP under in-plane or three-dimensional stress states including shear non-linearity”. NASA/TM-2003-213530, 2004.
- [11] Sujian Huang Akhtar S. Khan. “*Continuum theory of plasticity*”. Wiley Europe, 1995.
- [12] Danesi R. Luccioni B., Oller S. “Coupled plastic-damaged model”. *Comp. Methods in Applied Mechanics and Engineering*, Vol.129, pp 81–89, 1996.
- [13] Bažant, Z.P., Oh, B.H. “Crack band theory for fracture of concrete”. *Materials and Structures (RILEM, Paris)* Vol.16, pp 155-177, 1983.
- [14] S.T. Pinho, L.Iannucci, P.Robinson. “Physically based failure models and criteria for laminated fibre-reinforced composites with emphasis on the fibre kinking. Part II: FE implementation”. *Composite Part A: Applied Science and Manufacturing*, Vol.37, pp 766-777, 2005.